Biologically recycled continental iron is a major component in banded iron formations

Weiqiang Li[a,b,c,1], Brian L. Beard[a,b], and Clark M. Johnson[a,b]

[a]Department of Geoscience, University of Wisconsin-Madison, Madison, WI 53706; [b]NASA Astrobiology Institute, Madison, WI 53706; and [c]State Key Laboratory for Mineral Deposits Research, School of Earth Sciences and Engineering, Nanjing University, Nanjing 210093, People's Republic of China

Edited by Donald E. Canfield, Institute of Biology and Nordic Center for Earth Evolution, University of Southern Denmark, Odense, Denmark, and approved June 2, 2015 (received for review March 20, 2015)

Banded iron formations (BIFs) record a time of extensive Fe deposition in the Precambrian oceans, but the sources and pathways for metals in BIFs remain controversial. Here, we present Fe- and Nd-isotope data that indicate two sources of Fe for the large BIF units deposited 2.5 billion y ago. High-ε_{Nd} and -δ^{56}Fe signatures in some BIF samples record a hydrothermal component, but correlated decreases in ε_{Nd}- and δ^{56}Fe values reflect contributions from a continental component. The continental Fe source is best explained by Fe mobilization on the continental margin by microbial dissimilatory iron reduction (DIR) and confirms for the first time, to our knowledge, a microbially driven Fe shuttle for the largest BIFs on Earth. Detailed sampling at various scales shows that the proportions of hydrothermal and continental Fe sources were invariant over periods of 10^0–10^3 y, indicating that there was no seasonal control, although Fe sources varied on longer timescales of 10^5–10^6 y, suggesting a control by marine basin circulation. These results show that Fe sources and pathways for BIFs reflect the interplay between abiologic (hydrothermal) and biologic processes, where the latter reflects DIR that operated on a basin-wide scale in the Archean.

BIF | DIR | iron shuttle | Nd isotope | Fe isotope

Banded iron formations (BIFs) are Precambrian chemical marine sedimentary rocks that represent the major source of Fe used in today's society. Early studies suggested a continental source of Fe for BIFs (1, 2), although direct riverine input of Fe has been questioned because of the low-detritus components in the large superior-type BIFs (3). The discovery of midocean ridge (MOR) hydrothermal systems in the 1970s and the similarity of certain rare earth element (REE) signatures (e.g., positive Eu anomaly) between BIFs and MOR hydrothermal fluids led to a commonly accepted model, where BIFs were formed by oxidation of hydrothermally sourced aqueous Fe(II) (4–9). More recent work, particularly the combination of Nd isotopes and REEs, suggests a more complex origin for REEs in BIFs, where a significant component is sourced to the continents (10–14). Interpretations of Fe sources for BIFs using REE patterns and Nd-isotope ratios are, however, based on the underlying assumption that REEs and Fe pathways were coupled during transport and deposition of materials for BIFs, although this assumption has not been independently tested.

Deposition of BIFs requires the ancient oceans to be sufficiently reduced to allow transport of large quantities of aqueous Fe(II) but additionally, allow an oxidizing step to form insoluble Fe(III) oxides/hydroxides, and this combination indicates that BIFs likely record a vigorous Fe redox cycle, which could induce significant Fe-isotope fractionation between ferric and ferrous phases or aqueous species (15). The pathways by which Fe is deposited as BIFs have been studied in detail using stable Fe isotopes, but no consensus exists for explaining the wide range in measured δ^{56}Fe values (−2.5‰ to +1.5‰). Some studies have interpreted the negative δ^{56}Fe values of BIFs to reflect partial oxidation of hydrothermal Fe(II) (6, 16, 17), whereas others have proposed that the negative δ^{56}Fe values in BIFs reflect microbial dissimilatory iron reduction (DIR) in precursor BIF sediment before lithification (15, 18, 19). Difficulties in models that invoke partial oxidation of hydrothermal Fe(II) include the fact that only small quantities of Fe that has low-δ^{56}Fe values are produced by such a process, which is problematic for explaining Fe-rich rocks, such as BIFs. The DIR model may explain small-scale Fe-isotope variability in BIFs (20), but local recycling of Fe by DIR cannot well explain the changes in δ^{56}Fe values of BIFs on stratigraphic scales, unless a mechanism is found to transport large quantities of DIR-generated Fe on a basin-wide scale. An alternative mechanism to explain the low-δ^{56}Fe values in Archean marine sedimentary rocks has been put forth by Severmann et al. (21) based on studies of microbially generated Fe in the modern Black Sea, where aqueous Fe(II) produced by DIR on the shelf is delivered to the deeper basin by an "iron shuttle", trapped as sulfide, and precipitated as low-δ^{56}Fe pyrite. Although the benthic microbial Fe shuttle focused on the origin of pyrite in Archean shales (21), it offers a possible model for explaining the low-δ^{56}Fe superior-type BIFs.

Here, we address the question of Fe sources and pathways for BIFs by combining stable Fe isotopes with radiogenic Nd isotopes as well as REE measurements to test proposals that Fe in BIFs was hydrothermally sourced as well as evaluate proposals that a DIR-generated iron shuttle was important in BIF genesis. Radiogenic Nd-isotope ratios are used, because they are a sensitive discriminant of continental vs. oceanic sources but are not fractionated during deposition or dissolution of Fe oxides. Analysis of the first combined Fe–Nd-isotope dataset for BIFs, to our knowledge, leads us to a dual-source model for Fe in BIFs, including a hydrothermal component that has mantle-like Fe- and Nd-isotope signatures and a continental component that contains crustal Nd and isotopically light Fe derived from microbial iron shuttle. Our results confirm the arguments in previous REE and Nd-isotope work (10–13) that the Precambrian oceans were dynamic, where oscillations of ancient ocean environments caused

Significance

Combined Fe- and Nd-isotope signatures suggest that banded iron formations (BIFs) contain a major component of continentally derived iron that was mobilized by microbial iron reduction followed by transport through an iron shuttle to the site of BIF formation in deep basin environments. This Fe source is in addition to the widely accepted submarine hydrothermal source of Fe in BIFs, and the two sources of Fe may be comparable in importance, although their proportions change over time dependent on basin-scale circulation.

Author contributions: W.L., B.L.B., and C.M.J. designed research, performed research, analyzed data, and wrote the paper.

The authors declare no conflict of interest.

This article is a PNAS Direct Submission.

[1]To whom correspondence should be addressed. Email: liweiqiang@nju.edu.cn.

This article contains supporting information online at www.pnas.org/lookup/suppl/doi:10.1073/pnas.1505515112/-/DCSupplemental.

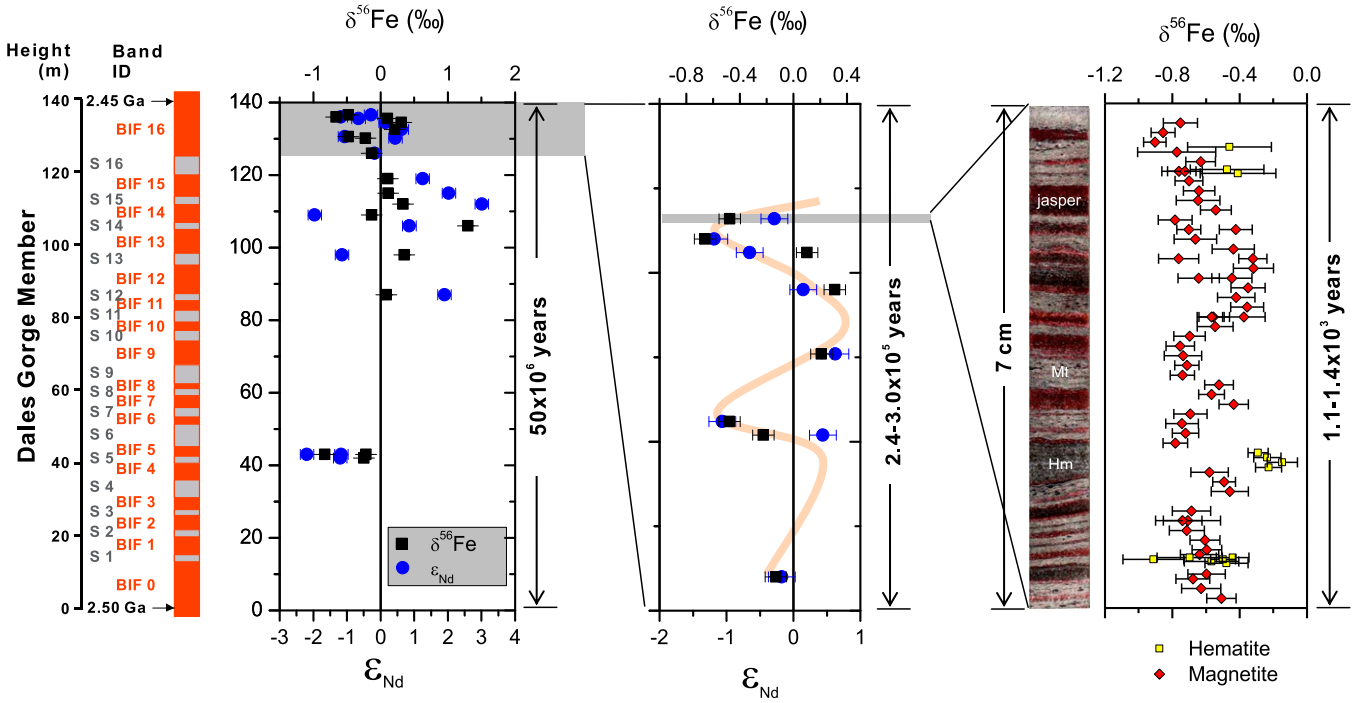

Fig. 1. Variation in Nd- and Fe-isotope compositions in the Dales Gorge member BIF sampled over different length and timescales. (*Left* and *Center*) Coupled Nd- and Fe-isotope data are from bulk sample solution analyses, and (*Right*) Fe-isotope data of hematite and magnetite are from in situ laser ablation analysis. The absolute age (2.50–2.45 Ga) and duration [50 million years (My)] of the Dale Gorge member BIF are suggested in ref. 24. The durations of BIF macroband 16 and the 7-cm drill core sample are estimated using a sedimentation rate of 50–63 m/Ma based on assuming that the finest scale banding (microbands) reflects annual or varve-like bands (*SI Appendix*, section 3); this assumption produces a sedimentation rate similar to that calculated using the total sediment thickness of a 50-My depositional interval.

secular changes in mixing ratios between hydrothermal and continental components.

Samples and Isotopic Results

We focus on the Dales Gorge member of the 2.5-gigaanum (Ga) age Brockman Iron Formation (Hamersley Basin, Western Australia, Australia), the world's most extensive superior-type BIF that represents the climax of BIF deposition in the geologic record (6, 7). The BIF samples analyzed in this study come from the type section diamond drill core for the Dales Gorge member (22, 23) (*SI Appendix*, Fig. S1). The depositional age of the Dales Gorge member is between 2.50 and 2.45 Ga (24). The Dales Gorge member is ∼160- to 140-m thick, consisting of 17 iron-rich, meter-scale macrobands and 16 shale macrobands, named BIF0–BIF16 and S1–S16, respectively (Fig. 1), and preserved sections reflect deposition in deep water conditions. The meter-scale, iron-rich macrobands are each composed of centimeter-scale, iron-rich mesobands (Fig. 1), which in turn, contain numerous submillimeter microbands (22). Iron-isotope compositions were measured at various sample scales from bulk (∼300-mg samples) measurements on the same aliquot used for Nd and REE analysis by isotope dilution mass spectrometry for mesoband samples in different macrobands to in situ analysis of Fe-isotope ratios and REE contents using femtosecond laser ablation (20) for microbands (methods details are in *Materials and Methods* and *SI Appendix*). Measured Fe- and Nd-isotope compositions reveal a large variation in both isotope systems: from −0.83‰ to +1.30‰ in δ^{56}Fe and −2.2 to +3.0 in ε_{Nd} (Fig. 1 and *SI Appendix*, Table S1). Between macrobands and within a macroband (e.g., BIF16), Fe- and Nd-isotope compositions oscillate over meter scales along the drill core (Fig. 1). In contrast, there is limited variation (<±0.2‰) in δ^{56}Fe values among microbands over centimeter scales of drill core depth (Fig. 1). Overall, there is a broad positive correlation between the δ^{56}Fe and ε_{Nd}-values (Figs. 1 and 2).

Discussion

The spread in Nd-isotope compositions of the BIF samples cannot be explained by the effects of siliciclastic contamination or hydrothermal alteration/metamorphism. Aluminum contents measured on the same aliquot used for REE and Nd-isotope analysis are very low, generally less than 0.4 grams per 100 grams (wt.%) Al_2O_3 (exceptions are two samples at 0.6 and 1.4 wt.%) (*SI Appendix*, Table S1), and there is no correlation between Al contents and Nd-isotope compositions, indicating that the negative ε_{Nd}-values do not reflect physical contamination with continental detritus. Previous Sm–Nd-isotope work on the Brockman Iron Formation suggested that secondary hydrothermal or metamorphic effects modified the Sm–Nd-isotope systematics after deposition (25). It is difficult, however, to envision a process at 2.1 Ga that homogenized $^{143}Nd/^{144}Nd$ ratios in BIF and shale samples at a stratigraphic scale but did not homogenize REE patterns, including $^{147}Sm/^{144}Nd$ ratios (Fig. 3). Although the Dales Gorge member BIF samples plot along a 2.1-Ga $^{143}Nd/^{144}Nd$–$^{147}Sm/^{144}Nd$ isochron in the study by Alibert and McCulloch (25), samples of the slightly older Marra Mamba BIF of the Hamersley Group plot along a $^{143}Nd/^{144}Nd$–$^{147}Sm/^{144}Nd$ reference isochron that corresponds to an age of 2.6 Ga (25), which is consistent with the depositional age, and a later metamorphic event should have affected both the Dales Gorge and the Marra Mamba BIFs.

Evidence against a homogenizing metamorphic event for the Dales Gorge member comes from in situ O-isotope analyses, which identified a substantial portion of low-δ^{18}O primary iron oxides (hematite and low-Si magnetite), indicating insignificant or negligible resetting of O-isotope compositions in these minerals by hydrothermal or metamorphic events (20). Some studies have

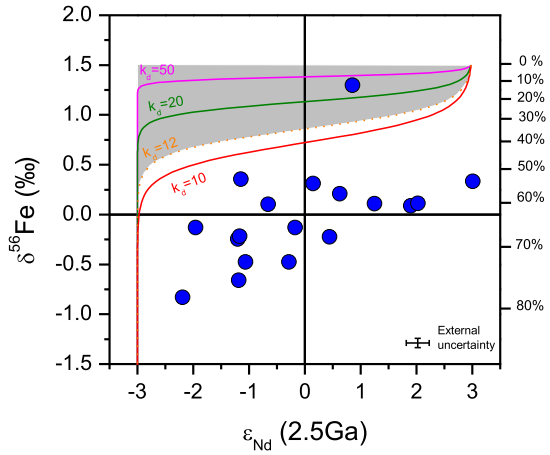

Fig. 2. Cross-plot of ε_{Nd}- and $\delta^{56}Fe$ values of drill core samples of the Dales Gorge member BIF (blue dots) and comparison with a Rayleigh model for partial oxidation of hydrothermal $Fe(II)_{aq}$. The Rayleigh model assumes a hydrothermal fluid that has an initial $\delta^{56}Fe$ value of 0‰ and a $\Delta^{56}Fe$ fractionation factor of +1.5‰ between $Fe(OH)_3$ and Fe(II); the degree of Fe(II) oxidation for a Rayleigh model is shown on the right axis. The model assumes a hydrothermal ε_{Nd}-value of +3 and a crustal ε_{Nd}-value of −3 for ambient seawater. K_d is defined as the Nd/Fe ratio between $Fe(OH)_3$ and solution, which is found to be 10^3–10^6 in laboratory experiments (28, 29) and 12–400 between modern vent fluid and near-vent Fe-rich sediments (31); the gray field encompasses solutions based on this K_d range. Details of the model are in *SI Appendix*.

argued for a secondary origin for hematite in some BIF samples based on petrographic evidence (26), but a secondary origin is not consistent with O-isotope results. Nevertheless, to test the possibility that the Nd-isotope compositions measured in the BIFs reflect a high-Nd secondary hydrothermal/metamorphic component, which has high-$\delta^{18}O$ values (20, 23), in situ REE analysis was performed and shows that the REE contents of hydrothermal or metamorphic magnetite are very low compared with low-$\delta^{18}O$ primary iron oxides (typically <0.3 vs. ∼1 ppm Nd) (*SI Appendix*, Fig. S6). Previous Nd-isotope studies of BIFs have not shown the fine-scale distribution of REEs in oxide-facies BIFs tied to in situ O-isotope measurements on different oxide generations, but the results obtained here and the arguments above indicate that the measured Nd-isotope compositions and REE contents represent the most primary low-temperature hematite and magnetite in the samples. Such a finding is critical for inferring seawater Nd-isotope signals in BIFs. As will be shown below, the $^{143}Nd/^{144}Nd$–$^{147}Sm/^{144}Nd$ correlation that led Alibert and McCulloch (25) to infer a 2.1-Ga age is, in fact, a mixing line between distinct Nd components.

Coupling of Nd and Fe Isotopes in BIFs. The large range in ε_{Nd}-values suggests mixing between a low-ε_{Nd} continental source and a high-ε_{Nd} mantle source for the REEs (27). The key question, however, is whether there was coupling between Nd and Fe or whether there was two end-member mixing for Fe as well; ε_{Nd}–$\delta^{56}Fe$ variations provide a test of the hypotheses that Fe was solely supplied from hydrothermal sources (4–7) and that the low-$\delta^{56}Fe$ values in BIFs are best explained by progressive partial oxidation of hydrothermal fluids (6, 16, 17). The relative slopes of ε_{Nd}–$\delta^{56}Fe$ variations (Fig. 2) are a function of the partition coefficients (K_d) for the REEs in iron oxides (28, 29) as well as the contrast in Nd-isotope compositions of the hydrothermal plume relative to the ambient ocean that had a continental Nd-isotope signature (30).

We assume a modest $\Delta^{56}Fe_{Fe(OH)3\text{-}Fe(II)aq}$ fractionation factor of +1.5‰, a hydrothermal fluid end member of $\delta^{56}Fe$ = 0‰, ε_{Nd} = +3, and Nd/Fe = 5×10^{-6} (grams per gram) (31); the ambient seawater component is assumed to have had zero initial $Fe(II)_{aq}$, Nd content of 1.15×10^{-10} g/g (32), and ε_{Nd}-value of −3. Our assumption of zero aqueous Fe(II) in ambient seawater maximizes the effects of the partial oxidation model, and hence, it is a conservative test for the proposal that negative $\delta^{56}Fe$ values are produced in the residual low-$Fe(II)_{aq}$ parts of the hydrothermal plume (6, 16). Although the K_d for REE partitioning into iron hydroxides can exceed 10^5 (typically >1,000) (28, 29), even a modest K_d of 10–50 shows that Nd contents of the hydrothermal plume will be rapidly depleted, such that mixing with ambient seawater will move the hydrothermal precipitates horizontally to the left in Fig. 2, failing to reproduce the observed ε_{Nd}–$\delta^{56}Fe$ variations. Use of higher, more realistic K_d values produces even poorer fits to the data. It is important to note that the model cannot start at a hydrothermal end member of $\delta^{56}Fe$ = 0 and ε_{Nd} = +3, because such an end member would imply a $\Delta^{56}Fe_{Fe(OH)3\text{-}Fe(II)aq}$ fractionation factor of zero, which violates the partial oxidation model, and would produce no change in $\delta^{56}Fe$ values of the remaining $Fe(II)_{aq}$. Use of a higher $\Delta^{56}Fe_{Fe(OH)3\text{-}Fe(II)aq}$ fractionation factor (+3‰) would produce even poorer fits to the observed ε_{Nd}–$\delta^{56}Fe$ variations (*SI Appendix*, Fig. S9). We conclude that the ε_{Nd}–$\delta^{56}Fe$ variations cannot be produced through partial oxidation of a single source of hydrothermally derived Fe but instead, reflect mixing of water masses that had distinct Fe- and Nd-isotope compositions (continental vs. mantle sources) in terms of dissolved $Fe(II)_{aq}$ and Nd followed by postmixing oxidation and precipitation as ferric oxyhydroxides, ultimately forming the BIFs.

Two Fe Sources for BIFs—a Microbial Fe Shuttle and Marine Hydrothermal Fluids. The ε_{Nd}–$\delta^{56}Fe$ variations indicate that the continentally sourced Fe has near-zero to negative $\delta^{56}Fe$ values down to −0.8‰, whereas the mantle/hydrothermally sourced Fe has slightly to strongly positive $\delta^{56}Fe$ values. The majority of samples

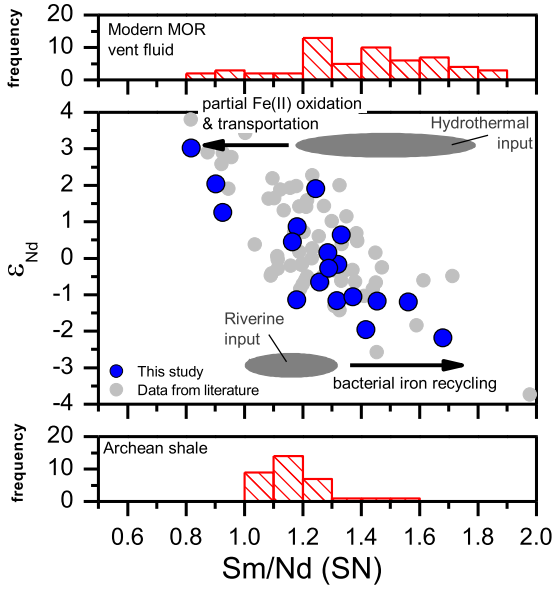

Fig. 3. Cross-plot of ε_{Nd}-values and shale-normalized Sm/Nd ratios of the Dales Gorge member BIF samples (this study; blue circles) and other BIF samples from Hamersley Basins (literature data; gray circles) as well as comparison with Sm/Nd distributions in Archean shales and modern MOR vent fluids. The observed ε_{Nd}–Sm/Nd trend suggests mixing between an end member that has low ε_{Nd}-values and high Sm/Nd, reflecting microbial iron cycling of continentally derived sediments, and an end member that has high ε_{Nd}-values and low Sm/Nd, reflecting partial oxidation of hydrothermal fluids

that have positive ε_{Nd}-values have δ^{56}Fe values that are slightly positive, indicating high extents of oxidation of hydrothermal Fe(II), although one highly positive δ^{56}Fe value is consistent with less oxidation (33). There are several possibilities for the origin of the low-δ^{56}Fe values for the continental (negative ε_{Nd}) component. Although modern riverine input could have negative δ^{56}Fe values (34) and dissolved Fe fluxes at ~2.5 Ga could have been sufficiently large for producing BIFs (35), a high-Fe dissolved riverine flux would be expected to have near-zero δ^{56}Fe values in a low-oxygen atmosphere, distinct from the low-δ^{56}Fe values and the very low-Fe contents of modern rivers (34, 36).

Given the difficulty in producing the low-ε_{Nd} and -δ^{56}Fe end member through precipitation from a hydrothermal plume and direct oxidation of dissolved riverine runoffs, a process is required to actively pump low-δ^{56}Fe $Fe(II)_{aq}$ into the Archean oceans from continental sources. Microbial DIR in coastal sediments is a mechanism that can release significant quantities of isotopically light $Fe(II)_{aq}$ to the oceans (15, 37, 38), and the model by Severmann et al. (21) for explaining low-δ^{56}Fe sedimentary pyrite by a DIR-driven Fe shuttle can be tested for its applicability to the Dales Gorge BIF based on the correlation between ε_{Nd}- and δ^{56}Fe values as well as Sm/Nd ratios. Support for a DIR shuttle as the source of the low-ε_{Nd} and -δ^{56}Fe component in the 2.5-Ga BIFs of this study comes from ε_{Nd}–Sm/Nd relations (Fig. 3). Microbial dissolution of iron hydroxides in modern marine sediments is accompanied by significant REE fractionation, where Fe(II)-rich pore waters contain significantly higher Sm/Nd ratios than bulk sediments (39), and this relation matches that seen for Sm/Nd ratios of the low-ε_{Nd} continental component relative to Sm/Nd ratios for Archean shales (Fig. 3). Importantly, Eu is preferentially mobilized during microbial diagenesis in marine sediments, producing positive Eu anomalies in pore fluids relative to bulk sediments (32, 40) and implying that the positive Eu anomaly may not be a unique indicator for a hydrothermal source for BIFs as previously thought (4, 5, 41). For the hydrothermal component, ε_{Nd}–Sm/Nd relations indicate low Sm/Nd ratios (Fig. 3), which likely reflect the effect of Fe(III) hydroxide precipitation given the fact that both laboratory experiments and field studies have shown that adsorption to particulate Fe(III) hydroxide fractionates REEs and that Sm is more strongly adsorbed onto Fe(III) particulates than Nd (28, 42), decreasing the Sm/Nd ratio in the remaining solution (Fig. 3). In short, the observed REE data (Eu anomaly and Sm/Nd ratio) are consistent with the proposed mixing model between two end members with fractionated REE signatures; this proposal may be tested through additional REE analysis, including Y determinations, although such an approach was not possible in this study because of measurement of the REEs by the isotope dilution method on the same aliquot measured for Fe and Nd isotopes.

Synthesizing the Nd- and Fe-isotope data and REE signatures, we propose a dual-source model for BIF genesis (Fig. 4*C*), where biologically recycled continental Fe and hydrothermal Fe from MOR systems both contributed as sources to BIFs. In the coastal region, Fe was sourced to continental runoff, and oxidation of aqueous Fe(II) produced Fe(III) oxyhydroxides that settled in a proximal continental shelf setting. Meanwhile, detritus and colloids brought by runoffs were efficiently removed by gravity settling and salt-induced coagulation (ref. 32 and references therein). Oxidation of riverine Fe(II) could have occurred through either oxygenic photosynthesis or Fe(II)-oxidizing, anoxygenic phototrophs (43, 44). Primary production of organic C and riverine supply of nutrients, such as P, along with Fe(III) oxyhydroxides would support DIR (45) in the proximal continental shelf. Export of Fe to the deep basin by a microbial Fe shuttle occurred at least initially through aqueous Fe(II) generated by DIR, and remobilization of the REEs by DIR-induced dissolution of Fe(III) oxyhydroxides produced the positive Eu anomalies and high Sm/Nd ratios that

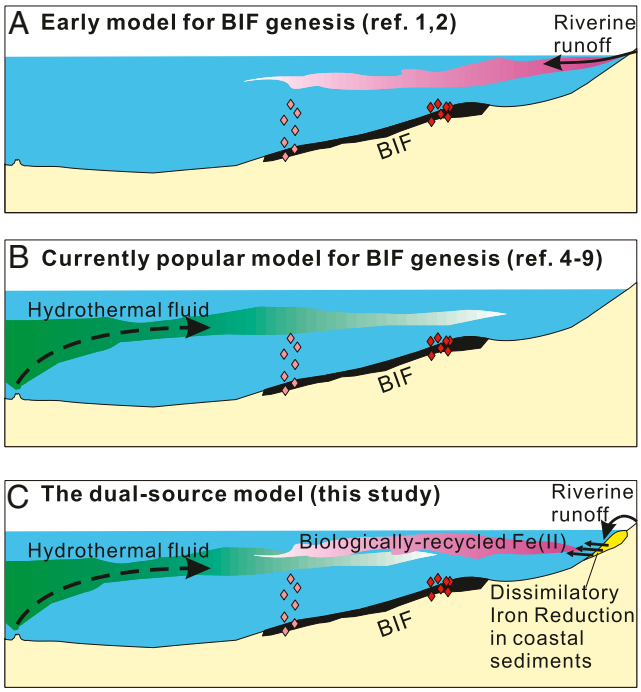

Fig. 4. Cartoons showing the genesis models for BIFs. (*A*) The hypothesis proposed by early studies that Fe in BIFs was originated from continental weathering and brought to the oceans by riverine inputs. (*B*) The model widely accepted by current workers that Fe in BIFs originated from hydrothermal fluids from MORs. (*C*) A previously unidentified dual-source model proposed here based on the new combined Nd–Fe data of this study that emphasize the continental sources of Fe derived from coastal sediments through microbial iron recycling.

are characteristic of the low-ε_{Nd} and -δ^{56}Fe component (Fig. 4*C*). These components ultimately mixed with diluted hydrothermal fluids that were sourced to the open ocean at different proportions, reoxidized (presumably in the photic zone), and precipitated as BIF precursors (Fig. 4*C*). Our model differs from the commonly held view that MOR hydrothermal fluids are the sole Fe source for BIFs (Fig. 4*B*), which cannot explain the spread in ε_{Nd} and coupling of Fe- and Nd-isotope compositions. Our model also differs from the early hypothesis that BIFs were formed by direct precipitation of continental Fe brought to the oceans through riverine inputs (Fig. 4*A*), which cannot explain the low-δ^{56}Fe values and ε_{Nd}–Sm/Nd relations in the BIF samples analyzed here. In addition, the DIR mechanism in the dual-source model decouples the continental isotopic signal from siliciclastic debris by mobilization by DIR and hence, also addresses the issue of low detrital contents in BIFs that have continental Nd isotopic signatures.

The DIR-driven Fe shuttle, which transports low-δ^{56}Fe iron to the deeper parts of the basin, should produce a complementary high-δ^{56}Fe pool of residual Fe in the proximal continental shelf. In the case of the Hamersley Basin, however, there are no proximal equivalents preserved, and the Dales Gorge member only provides a view of the deep basin setting. Iron-isotope data from the Kuruman Iron Formation (South Africa), which is correlative with the Brockman Iron Formation (9), provide support for a proximal high-δ^{56}Fe iron pool. Investigations by Heimann et al. (19) on the Kuruman Iron Formation reveal that samples from drill core (WB-98) of proximal sediments have consistently higher δ^{56}Fe values that those from drill core (AD-5) of distal sediments. Broadly, therefore, the Fe-isotope data of the Hamersley–Transvaal

basin are consistent with the geographic trends expected for a DIR-driven Fe shuttle.

Implications for Archean Ocean Environments. The range and distribution of ε_{Nd}-values in the BIF samples (Fig. 3) suggest that the amount of continental Fe recycled by DIR processes was comparable with the amount of Fe provided by MOR hydrothermal activity in the ocean at 2.5 Ga, at least for the BIFs in the Hamersley Group. To fuel such large-scale Fe recycling by DIR, a high primary productivity was required to generate sufficient amounts of organic carbon in coastal sediments (45). Identification of biologically recycled continental Fe as a major component in BIFs, therefore, attests to a vigorous microbial ecosystem in the late Archean ocean, where both Fe(II)-oxidizing and Fe(III)-reducing microbes thrived in the water column and soft sediment, respectively (43, 44). An active role for large-scale transport of Fe by DIR during BIF genesis at 2.5 Ga reflects relatively low-oxygen and -sulfide contents in the majority of the water column at this time, allowing transport of Fe as aqueous Fe(II), which would not be possible in the presence of high dissolved sulfide. Moreover, a major role for DIR in marine ecosystems at this time is consistent with the deeply rooted nature of Fe reduction metabolisms based on molecular phylogeny (46).

Demonstration of the dual sources of Fe for BIFs, one hydrothermal and one DIR-driven Fe shuttle from continental shelves, raises the question of the timescales over which such sources could have operated. It has been proposed, for example, that Fe(III) oxides in BIFs may be produced by photosynthetic oxidation of $Fe(II)_{aq}$ (44, 47), which in turn, might indicate seasonal variations that correlate with light intensity. At the smallest scale of banding, the submillimeter microbands that have been interpreted to represent annual varve-like layers (48, 49), in situ Fe-isotope analyses in this study show relatively small variation over timescales of $\sim 10^3$ y (Fig. 1). These results suggest that the DIR-driven Fe shuttle did not respond to seasonal changes in photosynthetic primary productivity, such as the amount of organic carbon production, at least from the perspective of the site of BIF deposition for the samples studied here. In contrast, at the scale of individual macrobands, which represent periods of $\sim 10^5$ y, Fe sources were clearly variable, as shown, for example, by macrosampling of BIF16 (Fig. 1). Over the ~50-My period represented by the entire Dales Gorge member (24), the balance between hydrothermal and continental DIR Fe sources also varied (Fig. 1). We conclude that the relative proportions of DIR and hydrothermal Fe sources recorded in BIF deposition were controlled by long-timescale changes that reflect variability in basin-wide circulation changes on the order of 10^5–10^6 y. It is possible that basin-wide sampling transects might record different scales of isotopic variability depending on conditions that affected the proportion of DIR- and hydrothermally sourced Fe. Nevertheless, the combined Fe- and Nd-isotope analysis indicates that BIFs formed from two sources of Fe and that an active DIR-driven Fe shuttle was operating at 2.5 Ga.

Materials and Methods

Small chips (typically 200–500 mg) were cut from the diamond drill core DDH-47A for bulk rock analyses. Sample digestion and ion exchange chromatography were performed using doubly distilled acids in a clean chemistry room. Bulk rock Neodymium isotope compositions were measured using a VG Instruments Sector 54 Thermal Ionization Mass Spectrometer. Bulk rock REEs were determined by isotope dilution mass spectrometry (IDMS) using a Micromass IsoProbe multi-collector inductively-coupled plasma mass spectrometer (MC-ICP-MS). Iron-isotope measurements were conducted using a Micromass IsoProbe MC-ICP-MS and an Aridus Desolvating Nebulizer with standard–sample–standard bracketing method (19); the external long-term reproducibility (2 SD) for δ^{56}Fe measurements using this method is ±0.08‰.

Centimeter- or subcentimeter-sized samples were cut from the diamond drill core DDH-47A and were embedded into 1-in-round epoxy plugs for in situ Fe-isotope and REE analyses. In situ analyses were done based on detailed back scattered electron (BSE) images (*SI Appendix*, Fig. S2). In situ Fe-isotope analysis was done using a femtosecond laser ablation (fs-LA) MC-ICP-MS system that consists of a femtosecond source laser that produces an output 266-nm beam, a Photon-Machines Beam-Delivery System, a Photon-Machines HelEX Ablation Cell, and a Micromass IsoProbe MC-ICP-MS (20). A standard–sample–standard bracketing method was used for mass bias and instrument drift correction. A magnetite in-house standard and a hematite in-house standard were used as the matrix-matching standards for fs-LA Fe-isotope analysis. External precision (reproducibility) of the fs-LA analysis was better than ±0.2‰ (2 SD) in δ^{56}Fe (20). In situ REE analysis was done using a system that consists of a Photon-Machines femtosecond laser and an Nu Plasma II MC-ICP-MS with multiple ion counting settings. More detailed explanations of the methods can be found in *SI Appendix*, section 2.

ACKNOWLEDGMENTS. This study benefited from discussions with Xinyuan Zheng, who also provided the compiled rare earth element data for modern midocean ridge hydrothermal vent fluids, and reviews by Kurt Konhauser and Balz Kamber. This study was supported by the NASA Astrobiology Institute. W.L. was supported by the 1000 Talent Program of China.

1. Cloud P (1973) Paleoecological significance of the banded iron-formation. *Econ Geol* 68(7):1135–1143.
2. Lepp H, Goldich SS (1964) Origin of Precambrian iron formations. *Econ Geol* 59(6): 1025–1060.
3. Holland HD (1978) *The Chemistry of the Atmosphere and Oceans* (Wiley, New York).
4. Bau M, Möller P (1993) Rare earth element systematics of the chemically precipitated component in early precambrian iron formations and the evolution of the terrestrial atmosphere-hydrosphere-lithosphere system. *Geochim Cosmochim Acta* 57(10): 2239–2249.
5. Klein C, Beukes NJ (1989) Geochemistry and sedimentology of a facies transition from limstone to iron-formation deposition in the early Proterozoic Transvaal Supergroup, South Africa. *Econ Geol* 84(7):1733–1774.
6. Bekker A, et al. (2010) Iron formation: The sedimentary product of a complex interplay among mantle, tectonic, oceanic, and biospheric processes. *Econ Geol* 105(3): 467–508.
7. Klein C (2005) Some Precambrian banded iron-formations (BIFs) from around the world: Their age, geologic setting, mineralogy, metamorphism, geochemistry, and origins. *Am Mineral* 90(10):1473–1499.
8. Alexander BW, Bau M, Andersson P, Dulski P (2008) Continentally-derived solutes in shallow Archean seawater: Rare earth element and Nd isotope evidence in iron formation from the 2.9 Ga Pongola Supergroup, South Africa. *Geochim Cosmochim Acta* 72(2):378–394.
9. Beukes NJ, Gutzmer J (2008) Origin and paleoenvironmental significance of major iron formations at the Archean-Paleoproterozoic boundary. *Banded Iron Formation-Related High-Grade Iron Ore*, Reviews in Economic Geology, eds Hagemann SG, Rosiere C, Gutzmer J (Society of Economic Geologists, Inc., Beukes, NJ), Vol 15, pp 5–47.
10. Alexander BW, Bau M, Andersson P (2009) Neodymium isotopes in Archean seawater and implications for the marine Nd cycle in Earth's early oceans. *Earth Planet Sci Lett* 283(1–4):144–155.
11. Miller RG, O'Nions RK (1985) Source of Precambrian chemical and clastic sediments. *Nature* 314(6009):325–330.
12. Wang C, Zhang L, Dai Y, Li W (2014) Source characteristics of the ~2.5 Ga Wangjiazhuang Banded Iron Formation from the Wutai greenstone belt in the North China Craton: Evidence from neodymium isotopes. *J Asian Earth Sci* 93(0):288–300.
13. Haugaard R, Frei R, Stendal H, Konhauser K (2013) Petrology and geochemistry of the ~2.9 Ga Itilliarsuk banded iron formation and associated supracrustal rocks, West Greenland: Source characteristics and depositional environment. *Precambrian Res* 229(0):150–176.
14. Viehmann S, Hoffmann JE, Münker C, Bau M (2013) Decoupled Hf-Nd isotopes in Neoarchean seawater reveal weathering of emerged continents. *Geology* 42(2):115–118.
15. Johnson CM, Beard BL, Roden EE (2008) The iron isotope fingerprints of redox and biogeochemical cycling in modern and ancient Earth. *Annu Rev Earth Planet Sci* 36(1): 457–493.
16. Planavsky N, et al. (2012) Iron isotope composition of some Archean and Proterozoic iron formations. *Geochim Cosmochim Acta* 80:158–169.
17. Rouxel OJ, Bekker A, Edwards KJ (2005) Iron isotope constraints on the Archean and Paleoproterozoic ocean redox state. *Science* 307(5712):1088–1091.
18. Johnson CM, Ludois JM, Beard BL, Beukes NJ, Heimann A (2013) Iron formation carbonates: Paleoceanographic proxy or recorder of microbial diagenesis? *Geology* 41(11):1147–1150.
19. Heimann A, et al. (2010) Fe, C, and O isotope compositions of banded iron formation carbonates demonstrate a major role for dissimilatory iron reduction in ~2.5 Ga marine environments. *Earth Planet Sci Lett* 294(1-2):8–18.
20. Li W, et al. (2013) Contrasting behavior of oxygen and iron isotopes in banded iron formations revealed by in situ isotopic analysis. *Earth Planet Sci Lett* 384(0):132–143.
21. Severmann S, Lyons TW, Anbar A, McManus J, Gordon G (2008) Modern iron isotope perspective on the benthic iron shuttle and the redox evolution of ancient oceans. *Geology* 36(6):487–490.

22. Trendall AF, Blockley JG (1968) Stratigraphy of the Dales Gorge Member of the Brockman Iron formation in the Precambrian Hamersley Group of Western Australia. Geological Survey of Western Australia Annual Report for 1967, ed Davies AB (The Department of Mines Western Australia, Perth, Australia), pp 86–91.
23. Huberty JM, et al. (2012) Silician magnetite from the Dales Gorge Member of the Brockman Iron Formation, Hamersley Group, Western Australia. *Am Mineral* 97(1): 26–37.
24. Trendall AF, Compston W, Nelson DR, De Laeter JR, Bennett VC (2004) SHRIMP zircon ages constraining the depositional chronology of the Hamersley Group, Western Australia. *Aust J Earth Sci* 51(5):621–644.
25. Alibert C, McCulloch MT (1993) Rare earth element and neodymium isotopic compositions of the banded iron-formations and associated shales from Hamersley, western Australia. *Geochim Cosmochim Acta* 57(1):187–204.
26. Rasmussen B, Krapež B, Meier DB (2014) Replacement origin for hematite in 2.5 Ga banded iron formation: Evidence for postdepositional oxidation of iron-bearing minerals. *Geol Soc Am Bull* 126(3-4):438–446.
27. DePaolo DJ (1988) *Neodymium Isotope Geochemistry: An Introduction* (Springer, Heidelberg).
28. Koeppenkastrop D, De Carlo EH (1992) Sorption of rare-earth elements from seawater onto synthetic mineral particles: An experimental approach. *Chem Geol* 95(3–4):251–263.
29. Quinn KA, Byrne RH, Schijf J (2006) Sorption of yttrium and rare earth elements by amorphous ferric hydroxide: Influence of pH and ionic strength. *Mar Chem* 99(1–4): 128–150.
30. Piepgras DJ, Wasserburg GJ (1980) Neodymium isotopic variations in seawater. *Earth Planet Sci Lett* 50(1):128–138.
31. Olivarez AM, Owen RM (1989) REE/Fe variations in hydrothermal sediments: Implications for the REE content of seawater. *Geochim Cosmochim Acta* 53(3):757–762.
32. Sholkovitz ER (1993) The geochemistry of rare earth elements in the Amazon River estuary. *Geochim Cosmochim Acta* 57(10):2181–2190.
33. Czaja AD, et al. (2012) Evidence for free oxygen in the Neoarchean ocean based on coupled iron-molybdenum isotope fractionation. *Geochim Cosmochim Acta* 86:118–137.
34. Fantle MS, DePaolo DJ (2004) Iron isotopic fractionation during continental weathering. *Earth Planet Sci Lett* 228(3-4):547–562.
35. Holland HD (1984) *The Chemical Evolution of the Atmosphere and Oceans* (Princeton Univ Press, Princeton).
36. Yamaguchi KE, Johnson CM, Beard BL, Ohmoto H (2005) Biogeochemical cycling of iron in the Archean-Paleoproterozoic Earth: Constraints from iron isotope variations in sedimentary rocks from the Kaapvaal and Pilbara Cratons. *Chem Geol* 218(1-2):135–169.
37. Severmann S, Johnson CM, Beard BL, McManus J (2006) The effect of early diagenesis on the Fe isotope compositions of porewaters and authigenic minerals in continental margin sediments. *Geochim Cosmochim Acta* 70(8):2006–2022.
38. Bergquist BA, Boyle EA (2006) Iron isotopes in the Amazon River system: Weathering and transport signatures. *Earth Planet Sci Lett* 248(1-2):54–68.
39. Haley BA, Klinkhammer GP, McManus J (2004) Rare earth elements in pore waters of marine sediments. *Geochim Cosmochim Acta* 68(6):1265–1279.
40. MacRae ND, Nesbitt HW, Kronberg BI (1992) Development of a positive Eu anomaly during diagenesis. *Earth Planet Sci Lett* 109(3–4):585–591.
41. Fryer BJ (1977) Rare earth evidence in iron-formations for changing Precambrian oxidation states. *Geochim Cosmochim Acta* 41(3):361–367.
42. Rudnicki MD, Elderfield H (1993) A chemical model of the buoyant and neutrally buoyant plume above the TAG vent field, 26 degrees N, Mid-Atlantic Ridge. *Geochim Cosmochim Acta* 57(13):2939–2957.
43. Czaja AD, et al. (2010) Iron and carbon isotope evidence for ecosystem and environmental diversity in the ~2.7 to 2.5 Ga Hamersley Province, Western Australia. *Earth Planet Sci Lett* 292(1-2):170–180.
44. Kappler A, Pasquero C, Konhauser KO, Newman DK (2005) Deposition of banded iron formations by anoxygenic phototrophic Fe(II)-oxidizing bacteria. *Geology* 33(11):865–868.
45. Konhauser KO, Newman DK, Kappler A (2005) The potential significance of microbial Fe(III)-reduction during Precambrian banded iron formations. *Geobiology* 3(3):167–177.
46. Weber KA, Achenbach LA, Coates JD (2006) Microorganisms pumping iron: Anaerobic microbial iron oxidation and reduction. *Nat Rev Microbiol* 4(10):752–764.
47. Posth NR, Hegler F, Konhauser KO, Kappler A (2008) Alternating Si and Fe deposition caused by temperature fluctuations in Precambrian oceans. *Nat Geosci* 1(10):703–708.
48. Morris RC (1993) Genetic modelling for banded iron-formation of the Hamersley Group, Pilbara Craton, Western Australia. *Precambrian Res* 60(1–4):243–286.
49. Drever JI (1974) Geochemical Model for the Origin of Precambrian Banded Iron Formations. *Geol Soc Am Bull* 85(7):1099–1106.